TRENDS IN SCIENCES 2025; 22(11): 10778
https://doi.org/10.48048/tis.2025.10778 RESEARCH ARTICLE

Pineapple Waste Cellulose Hydrogel: A Sustainable Absorbent for Drug Delivery System

Heri Satria*, Kamisah Delilawati Pandiangan, Hapin Afriyani, Diska Indah Alista, Arifah Rara Afiria and Febiana Nabila

Department of Chemistry, Faculty of Mathematics and Natural Sciences, University of Lampung, Bandar Lampung 35145, Indonesia

(*Corresponding author's e-mail: heri.satria@fmipa.unila.ac.id)

Received: 26 May 2025, Revised: 7 June 2025, Accepted: 20 June 2025, Published: 5 August 2025

Abstract

Cellulose-based hydrogels are valuable biomaterials used in drug delivery systems. Cellulose, a biopolymer found in sources like agricultural waste, is abundant in countries such as Indonesia. PT Bromelain Enzyme in Lampung Province generates roughly 20 tons of cellulose-rich pineapple core waste annually from bromelain extraction, providing significant raw material for hydrogel production. This study explored the feasibility of using this waste for synthesizing hydrogels and assessing their potential as drug-delivery agents through various experiments. TAPPI methods for composition analysis revealed 38.5% cellulose, 25.05% hemicellulose and 12.99% lignin in the waste. The isolation of mangrove actinomycetes on ISP 2 medium identified the ActM-DMB 7 isolate, which displays high xylanolytic activity. This isolate was utilized in bio-pretreatment to remove amorphous portions, yielding highly crystalline cellulose with an increased crystallinity index from 16.68 to 33.35. Cellulose resizing showed a bimodal distribution of particle diameters at 0.657 and 1.832 µm. Hydrogel production utilized grafting, confirmed by FTIR analysis with characteristic N-H (3,183.14 cm^{-1}) and C=O (1,647.48 cm^{-1}) amide bands. The product was examined for absorption and delivery potential of ascorbic acid and amoxicillin, exhibiting a high swelling ratio (plateauing at ~34 Sg/g) and significant water retention over 10 h. The hydrogels efficiently absorbed and released ascorbic acid and amoxicillin, with amoxicillin showing antibacterial effects against *Escherichia coli* and *Staphylococcus aureus*. This research emphasizes valuing pineapple processing waste for sustainable, economically viable functional hydrogels for biomedical applications, including drug delivery, aligning with circular economy principles by transforming an industrial byproduct into a high-value material.

Keywords: Hydrogel, Cellulose, Actinomycetes, Poly-acrylamide, Ascorbic acid, Amoxicillin

Introduction

Bio-based materials continue to garner increasing interest due to their significant role in various biomedical applications, including tissue engineering, wound healing and drug delivery. Polysaccharides, which are long-chain biopolymeric carbohydrate molecules composed primarily of monosaccharide units, have emerged as promising bio-based materials [1]. These polymers offer substantial advantages in biomedical applications, as their inherent beneficial properties surpass those of synthetic alternatives. Among the diverse polysaccharides, cellulose is regarded as a fundamental natural biopolymer due to its widespread availability in nature [2].

Cellulose is a key component of lignocellulosic composites found in numerous agricultural wastes. Since the composite is arranged within a complex matrix, cellulose has a microfibril structure. This morphology enhances the mechanical properties, providing structural stability that facilitates modifications needed to fabricate advanced materials [3]. Furthermore, the chemical structure of cellulose allows for crosslinking with other molecules to form molecular networks [4]. The advantageous physical and

chemical properties make cellulose widely applicable in advanced healthcare materials, including hydrogels [5]. Using cellulose from agricultural waste for hydrogel synthesis significantly converts this byproduct into valuable materials, thus promoting 'waste-to-wealth' strategies.

One potential source of cellulose in Indonesia is PT Bromelain Enzyme, located in Lampung province. This company extracts bromelain enzyme from pineapple cores, which in turn produces a large quantity of pineapple core residue (approximately 20 tons each year) as waste. Notably, this significant residue currently remains unutilized. This residue is rich in cellulose [6] and therefore, offers the opportunity to use a sustainable source of cellulose needed for hydrogel production.

To enhance cellulose extraction from this residue, the researcher can employ a promising approach: An enzymatic process using actinomycete enzymes. These enzymes facilitate partial degradation of the polymer components within the residue, thereby simplifying cellulose separation [7,8]. This enzymatic process has demonstrated greater selectivity and efficiency in breaking down complex biomass structures than traditional chemical methods. Furthermore, enzyme-assisted extraction is considered more environmentally friendly and cost-effective while increasing the extracted cellulose yield and purity.

Despite its availability and natural characteristics, cellulose does not meet all requirements for direct use in drug delivery systems; therefore, modification is still necessary. In this context, grafting is recognized as the most widely used method for improving the properties of cellulose through chemical modification, with acrylamide being a hydrogel [9]. Hydrogel with significant potential in medicine is effectively synthesized through the well-established technique of grafting cellulose with acrylamide [10].

Cellulose-based hydrogels have the unique capability that the network form is desirable for self-healing capabilities and adjustable swelling ratios. The presence of their polar or charged functional groups is highly hydrophilic, enabling them to absorb water and swell in various environments. A high value in a swelling ratio of hydrogels, known for their permeability and biocompatibility, is particularly favored in medical applications [11,12]. Free hydroxyl groups also play a significant role in enhancing the hydrophilicity of the hydrogel, thus improving the water retention capacity of the material, which is critical for applications in drug delivery systems [13]. Moreover, hydrogels can act as matrices that encapsulate molecules like small peptides, proteins and nucleotides, showcasing broad applicability due to their ability to release entrapped compounds in a controlled manner [14].

This research aims to synthesize hydrogels by grafting cellulose derived from pineapple core waste with polyacrylamide. The enhanced absorption properties and potential applications for vitamin C delivery and antibiotics were investigated. The significance of this research lies in its potential to develop hydrogels from environmentally problematic industrial wastes and it simultaneously offers an innovative contribution to health-related applications.

Materials and methods

Materials

Pineapple core waste was collected from PT Bromelain Enzyme, Lampung, Indonesia. Laboratory grade chemicals such as ISP-2, Yeast Extract Mannitol Broth (YMB) media, Muller-Hinton Agar (MHA), amoxicillin, birchwood xylan, congo red, sulfuric acid (H_2SO_4) 72%, Acrylamide (AAm), N, N'-methylenebisacrylamide (MBA), 0.2 N Na_2HPO_4-NaH_2PO_4 buffer solution, ammonium persulfate (APS), ethanol, methanol, aceton, distilled water were purchased from diverse of commercial suppliers. *E. coli* and *S. aureus* were obtained from the Indonesian Culture Collection (Ina-CC), National Research and Innovation Agency (BRIN).

Compositional analysis of pineapple core waste

The pineapple core waste obtained was dried using an oven at 105 °C, then ground and sieved to get the sample with a particle size of 40 mesh. TAPPI standard methods were applied to determine its composition. Specifically, cellulose content was quantified using the standard method TAPPI T203 cm-99, hemicellulose content was determined following TAPPI T223 cm-84 and lignin content was assessed using TAPPI T222 om-02, with a subtle modification [15].

Screening of mangrove sludge actinomycetes isolate

Screening of actinomycetes isolates was carried out to obtain bacteria that have xylanolytic activity. The isolates were obtained from mangrove sludge collected from Dwi Mandapa Beach, Pesawaran, Lampung (−5.571883, 105.243494). Isolation and purification of actinomycetes were subsequently conducted by pour plates and single colony quadrant-streaking. The pure single colony isolate was tested on ISP-2 on two separate media. The first medium contains, 5 wt% of Birchwood xylan to investigate the presence of xylanolytic activity and the second medium contains Carboxy Methyl Cellulose (CMC) to investigate the presence of cellulolytic activity. The incubation period lasts 5 - 7 days at 37 °C before being treated with Congo red solution for 15 min to form a clear zone around the colony. The sample was rinsed with 1 M NaCl to enhance the visibility of the clear zone, making it easier to observe. The clear zone around the bacterial colony indicates xylanolytic and cellulolytic activity. The index of xylanolytic or cellulolytic activities was quantified by relating the diameter of the clear zone to the size of the colony.

Bio-pretreatment and cellulose purification

Biological pretreatment was performed using selected actinomycetes with xylanolytic activity to hydrolyze pineapple core waste. The optimization of hydrolysis time was conducted by hydrolyzing 50 wt% of the pineapple core waste with selected actinomycetes isolates in 250 mL of YMB medium. The medium composition included (wt%) 0.4 dextrose, 1.0 malt extract and 0.4 yeast extract. The hydrolysis process lasted for 9 days at 120 rpm. The initial pH of the medium was adjusted to 7.0 using a 0.2 N Na_2HPO_4-NaH_2PO_4 buffer solution [8]. After the process, the cellulose was washed with distilled water and filtered to remove residual bacterial cells [16]. The samples obtained were then characterized using an X-ray diffraction (XRD) instrument (PANalytical type Empyran). The crystallinity index of the sample was calculated according to the Segel method using Eq. (1).

$$CrI = \frac{I_{002} - I_{am}}{I_{002}} \times 100 \quad (1)$$

CrI is the crystallinity index, I_{002} is the maximum intensity of the crystalline peak (around $2\theta = 22° - 23°$) and I_{am} is the minimum intensity of the amorphous area.

Cellulase and xylanase assay

To obtain the crude enzyme, 10 mL of culture supernatant was collected and then centrifuged at 4 °C and 10,000 rpm for 10 min. The resulting clarified supernatant, representing the crude enzyme, was then used for subsequent assays. Cellulase and xylanase activities were quantified using established CMC-ase and xylanase assay protocols [17,18]. For CMC-ase activity, a 0.5 mL aliquot of the crude enzyme was reacted with 0.5 mL of 1% soluble CMC in 0.05 M sodium citrate buffer (pH 5.0) at 37 °C for 30 min. The reaction was subsequently terminated by the addition of 1.0 mL of 3,5-dinitro salicylic acid (DNS) reagent, followed by boiling at 95 °C for 15 min. The liberated reducing sugars, expressed as glucose equivalents, were then spectrophotometrically determined using the DNS method [19] against a glucose standard. One unit of CMC-ase activity (U/mL) was defined as the enzyme quantity releasing 1 μmol of glucose per min under the assay conditions. Xylanase activity was determined analogously, with 0.5 mL of crude xylanase enzyme filtrate incubated with 0.5 mL of 1% birch wood xylan in the same buffer. The reaction was stopped with DNS reagent and heated similarly. The released xylose was quantified spectrophotometrically using a xylose standard and one unit of xylanase activity (U/mL) was defined as the enzyme amount yielding 1 μmol of xylose per min.

Reduction of cellulose particle size

To reduce the particle size of the cellulose, the sample was subjected to partial acid hydrolysis and then followed by sonication. In the partial acid hydrolysis, an aliquot of 200 mL of 5 M H_2SO_4 was heated to 45 °C in a 500 mL Erlenmeyer flask and then 10 g of cellulose powder was added into the solution and hydrolyzed for 60 min. The suspension was centrifuged at 10,000 rpm for 10 min and then decanted. The precipitate was washed with distilled water and then neutralized using 5% Na_2CO_3 until the pH reached neutral (around 7,0). Subsequently, the sample was subjected to sonication treatment by diluting the sample using distilled water to a 5% concentration and sonicated at 40 kHz for 60 min.

The suspension sample was centrifuged at 10,000 rpm for 10 min, decanted and dried using a vacuum freeze dryer. The final product was characterized using a Particle Size Analyzer (PSA) model Beckman Coulter LS 13 320 to determine the particle size distribution of the sample.

Hydrogel preparation

A mass of 1 g of dry cellulose was placed into a three-necked flask with a condenser, thermometer and stirring rod. Distilled water was added to the cellulose to form a pulp and then heated at 95 °C for 30 min. Afterward, the temperature was lowered to 60 °C, 0.05 g of APS was added and the solution was stirred for 15 min. Subsequently, a mixture of 5 g of Aam and 5 mg of MBA dissolved in 40 mL of distilled water was added. The temperature was gradually increased to 70 °C and maintained for 3 h [20]. The resulting product was precipitated using ethanol and methanol and the precipitate was then refluxed with acetone for 1 h and then characterized using Agilent Technologies model Fourier Transform Infra-Red Spectroscopy (FTIR).

Determination of swelling capacity and water retention

The extent of hydrogel swelling was determined through gravimetric analysis of both dehydrated and hydrated samples. Initially, precisely weighed, thoroughly dried hydrogel was immersed in 50 mL of deionized water within a 100 mL beaker to reach equilibrium. The swollen hydrogel was carefully removed at predetermined time points and any superficial water was eliminated using absorbent filter paper. The weight of the water-absorbed hydrogel was then recorded using an analytical balance (GH-200, A&D weighing, Tokyo, Japan). Subsequently, to assess water retention, the equilibrated hydrogel was placed in petri dishes at ambient temperature and their weight was monitored at specific time intervals until a stable, saturated weight was achieved. The swelling ratio (Sg/g) and % of water retention can be calculated using the following Eqs. (2) - (3).

$$\text{Swelling ratio (Sg/g)} = \frac{W - W_0}{W_0} \quad (2)$$

$$\text{Water retention (\%)} = \frac{W_t - W_0}{W_d - W_0} \times 100 \quad (3)$$

W_t is the swollen hydrogel weight at time intervals, W_o is the weight of the dried hydrogel and W_d is the initial weight of the swollen hydrogel.

Absorption and release test of vitamin C (ascorbic acid/AAc) by hydrogel

The ability of the hydrogel to absorb and release AAc was evaluated through a series of experiments. A mass of 0.1 g of the dry hydrogel was soaked in 25 mL of a 100 mg/L AAc solution for varying durations of 4, 8, 12, 24 and 48 h. The absorbed vitamin C was then released by immersing the hydrogel in distilled water for 72 h. The released vitamin C was determined through iodometric titration by mixing the sample with 10 mL of 20% (v/v) H_2SO_4 and 1.0 mL of 10% (v/v) KI, then titrating with 0.002 M KIO_3 using 1% starch as an indicator. The titration utilized a KIO_3 solution where 1 mL was equivalent to 0.8806 mg of AAc ($C_6H_8O_6$) [21,22]. The release of AAc was assessed using a diffusion method, where the hydrogel was immersed in 25 mL of distilled water after absorbing vitamin C. The release time was measured based on the hydrogel optimal absorption duration and the change in AAc concentration in the solution was observed after 2, 4, 6, 8, 12, 18 and 24 h. Each sample was filtered and the released vitamin C content was quantified through iodometric titration as in the previous procedure. The Higuchi model was applied to the AAc release data by plotting the cumulative percentage of AAc released against the square root of time [23].

Bacterial inhibition test

The ability of the hydrogel to release antibiotics was evaluated using the Kirby-Bauer disk diffusion assay method with some modifications. A mass of 0.1 g of dry hydrogel sample was soaked in 1 mL of a series of concentrations of dilute amoxicillin (0, 25, 50 and 100 µg/mL) solution for 24 h. The swelling-hydrogel that absorbs amoxicillin was placed onto swabbing MHA with 24 h cultured *E. coli* and *S. aureus* [24].

Results and discussion

Composition of pineapple core waste

The main components of the sample are lignin, hemicellulose and cellulose with the relative composition as presented in **Figure 1**. As can be seen, cellulose is the component with the highest contribution

(38.50%), followed by hemicellulose (25.05%) and lignin (12.99%).

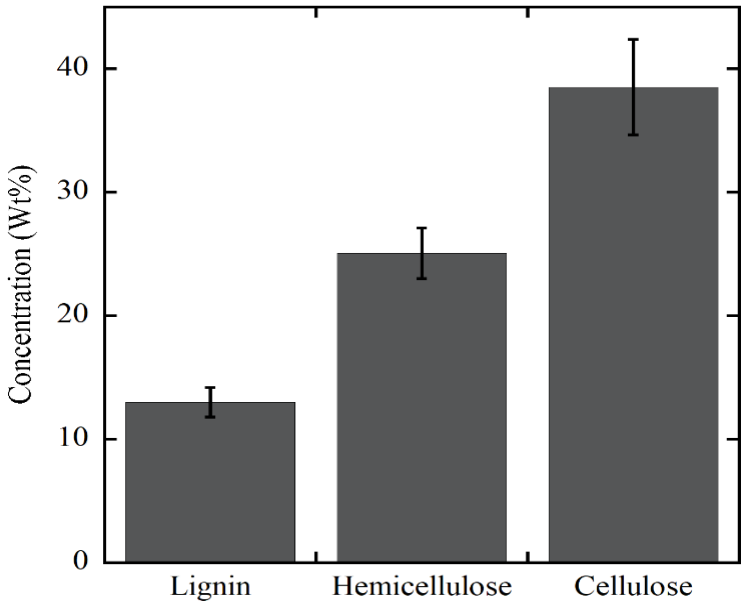

Figure 1 The main biopolymer components of pineapple core residue investigated in this study.

The pineapple core waste groups into non-wood material, which some researchers have examined and reported the content of cellulose in the range of 30% to 50%, hemicellulose 20% to 35% and 15% to 30% on a weight basis [25]. The composition variation is attributed to plant species, cultivation technique and geographical factors [26-29] concerning this variation in composition, the composition of the sample investigated in this study agrees with the results reported by others.

Mangrove sludge actinomycetes isolates

From screening experiments, one particular isolate with high xylanolytic and low cellulolytic activity was obtained and specified as ActM-DMB 7 isolate. This isolate was then tested for xylanolytic and cellulolytic activity, by cultivation experiment for five days on ISP-2 medium supplemented with 5 %w/v Birchwood xylan and CMC and visualized through Congo red staining to produce clear zones around the colonies, as indicated in **Figure 2**.

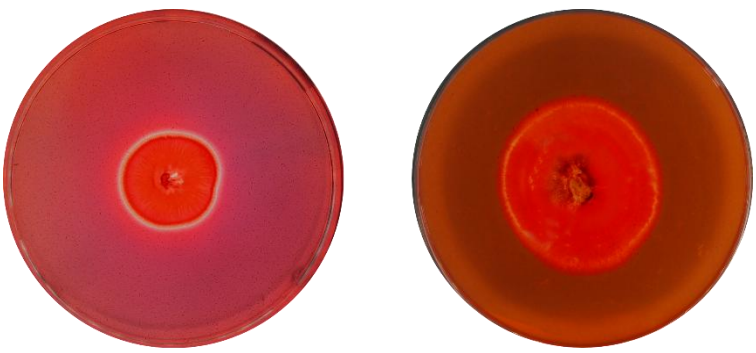

(a) **(b)**

Figure 2 The results of screening experiments to identify xylanolytic activity (a) and cellulolytic activity of ActM-DMB 7 isolate (b), using Congo red.

As can be observed in **Figure 2**, in both experiments the clear zone was observed, implying that the isolate has xylanolytic and cellulolytic activity. Based on the clear zone observed, it can be seen that the isolate tested has higher xylanolytic activity. For quantitative comparison, xylanolytic index and cellulolytic index were calculated relating the diameter of the clear zone to the size of the colony [30] and it was found the value of 1.054 for xylanolytic index and 1.003 for cellulolytic index. This xylanolytic index of ActM-DMB 7 demonstrates its ability to degrade hemicellulose effectively and therefore this isolate was then applied in bio-pretreatment experiment for hemicellulose degradation to facilitate cellulose liberation. Enzymatic activity is crucial as it plays a role in the depolymerization of hemicellulose, a key structural component that often encases cellulose fibers within lignocellulosic biomass. Previous studies have shown that the effective removal of hemicellulose can significantly enhance cellulose accessibility, making the process more efficient for subsequent applications, including hydrogel production [31].

Bio-pretreatment and cellulose purification

Bio-pretreatment aims to separate the cellulose from the pineapple core waste. For this purpose, a hydrolysis experiment was conducted for 9 days, then the xylanase and cellulase activity of ActM-DMB 7 were measured, as can be seen in **Figure 3**.

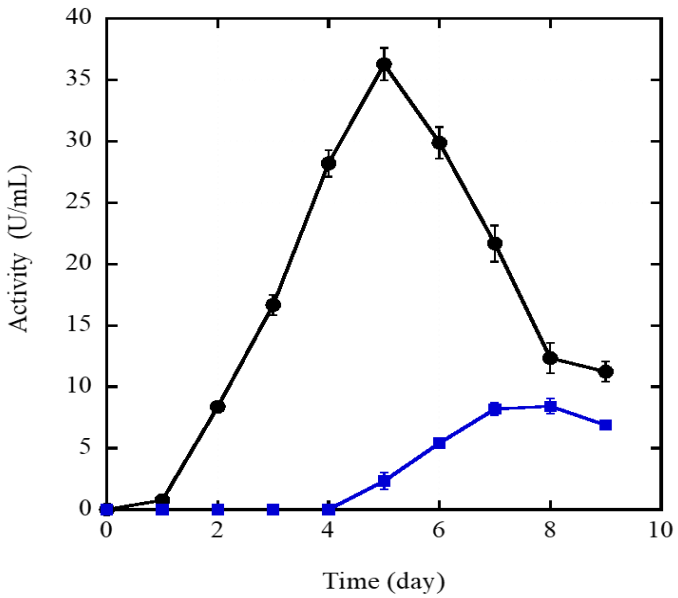

Figure 3 Xylanase and cellulase activity of ActM-DMB 7 isolate as a function of hydrolysis times.

Figure 3 illustrates the profile of xylanase and cellulase activity (U/mL) produced by the ActM-DMB 7 over a 9-day cultivation hydrolysis in YMB medium enriched with 45 wt% pineapple core waste. The results show that ActM-DMB7 displays a strong capability in the enzymatic degradation of hemicellulose, as evidenced by the pronounced xylanase activity observed from day 2 onward, reaching a peak of 36 (U/mL) on day 5. ActM-DMB 7 has ability to produce xylanase quickly and in large quantities, suggesting its significant potential as a valuable agent for bio-pretreatment, thereby facilitating cellulose extraction from lignocellulosic biomass. The preferential degradation of hemicellulose can significantly reduce the recalcitrant nature of the biomass, thereby facilitating downstream processes for cellulose extraction and utilization in hydrogel production [32,33].

Interestingly, despite significant xylanase production, the cellulase activity remained comparatively low, peaking at only 8 U/mL on day 8. This disparity could imply a strategic metabolic adaptation of ActM-DMB 7, prioritizing hemicellulose breakdown to enhance cellulose availability before further cellulolytic action occurs. Literature suggests that a focused approach to removing hemicellulose can lead to a more porous structure in the lignocellulosic

matrix, thereby improving enzymatic accessibility during subsequent hydrolysis stages [34,35].

Furthermore, the advantage of late-stage cellulase activity may hint at a sequential enzymatic action where xylanase primes the biomass, setting the stage for enhanced cellulolytic activity thereafter. This order aligns with the theory of enzymatic synergy, where combined xylanase and cellulase applications yield improved overall biomass degradation efficiency. Previous studies have demonstrated that such synergistic interactions yield better saccharification yields than cellulase alone [36]. Therefore, the observed high xylanase activity and relatively low cellulase activity support the selection of ActM-DMB 7 as a promising agent for biomass bio-pretreatment. Its ability to preferentially target hemicellulose, as evidenced by the earlier and higher production of xylanase, could lead to a more efficient and potentially less damaging pretreatment process for cellulose recovery from lignocellulosic biomass. The observed enzymatic activities provide a promising avenue for improving biomass (in this study is pineapple core waste) bio-pretreatment strategies that ultimately enhance the usability of derived cellulose in various biotechnological applications, including hydrogel production, rather than focusing only on fermentable sugar yields [37,38].

The order of xylanase and cellulase work one after the other to degrade biomass, emphasizing their synergistic importance in enabling the breakdown of complex lignocellulosic structures. The selective removal of the hemicellulose fraction from biomass, evidenced by weight loss, directly impacts the structural organization of the remaining material. In this study, the mass loss after bio-pretreatment was around 38%. This significant mass loss can be primarily attributed to the enzymatic degradation of the amorphous regions, which are more susceptible to enzymatic attack than cellulose densely packed crystalline regions. This condition aligns with previous findings indicating that enzymatic treatments preferentially cleave the amorphous portions of lignocellulose, thereby facilitating the exposure of the more crystalline portions to subsequent degradation processes [39,40]. The critical aspect is that cellulose structure consists of amorphous and crystalline regions, which play an essential role in its biochemical accessibility and the effective degradation of hemicellulose, as indicated by the xylanase activity, also aids in the liberation of these amorphous structures [41,42].

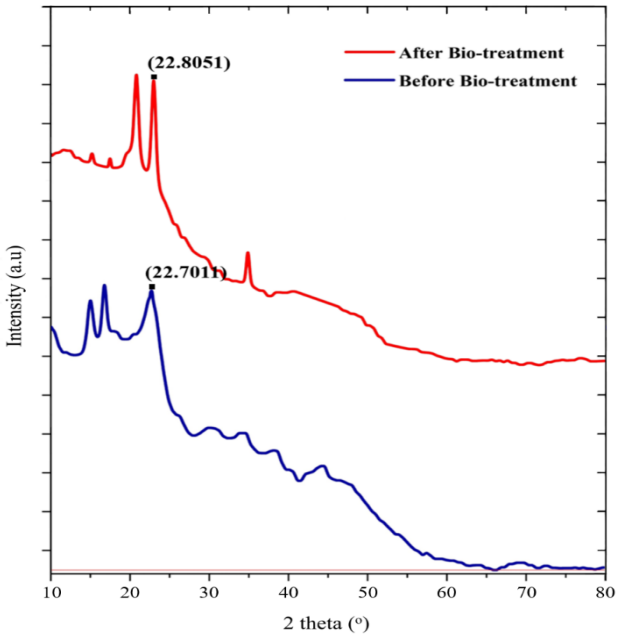

Figure 4 X-ray diffractograms of cellulose investigated (a) before and (b) after bio-pretreatment, illustrating changes in crystalline structure.

Changes in the cellulose crystalline structure due to bio-pretreatment were evident in the X-ray diffractograms (**Figure 4**). Peak identification, achieved by matching the 2-theta angle with literature data from the Joint Committee on Powder Diffraction Standards (JCPDS) for cellulose, identified the major peak in pre- and post-treated samples around 22.7° - 22.8°. This peak corresponds to cellulose type I (alpha-cellulose), as referenced by JCPDS 03-0289 [43]. However, a significant difference was observed in the crystallinity index (CrI), calculated using the Segal method (**Table 1**). The initial CrI value of the untreated sample was 16.86%, which increased substantially to 33.35% after biological treatment by the ActM-DMB 7 isolates.

This notable increase in CrI suggests that the bio-pretreatment process effectively removed amorphous components such as lignin and hemicellulose. This selective breakdown of amorphous regions leads to a relative enrichment of the more ordered crystalline cellulose. This finding aligns with observations by [44], who emphasized that the removal of lignin and hemicellulose can result in a CrI increase of 10% - 15%, depending on the method. Furthermore, the observed weight loss of 38% and the corresponding rise in crystallinity underscore the dual action of the enzymatic treatment: The removal of less ordered components and the consequent increase in the proportion of the more stable, albeit less enzymatically accessible, crystalline cellulose [45,46].

Table 1 Crystallinity Index (CrI) of pineapple core waste before and after bio-pretreatment, calculated using the Segal method based on I_{002} (intensity at $2\theta \approx 22° - 23°$) and Iam (intensity at $2\theta \approx 18°$), refer to Eq. (1).

Sample	I_{002}	I_{am}	CrI (%)
Before Bio-pretreatment	496.29	412.59	16.86
After Bio-pretreatment	637.20	424.70	33.35

Particle size of cellulose

Characterization of the sample through the PSA method revealed the particle size distribution shown in **Figure 5**. This figure indicates that the data informs a bimodal distribution with two distinct peaks in particle diameter at 0.657 and 1.832 μm. Observing a bimodal particle size distribution after mechanically resizing the cellulose derived from ActM-DMB 7 bio-pretreatment suggests a varied population of cellulose structures. The main peak at 0.657 μm reflects the presence of smaller particles, corresponding to the expected size of cellulose fibrils [47]. This finding confirms that the sonication step successfully reduced the cellulose size.

Conversely, the secondary peak at 1.832 μm points to the existence of larger particles, likely indicating cellulose agglomeration that occurred during processing or analysis. Aligning with the research of Mendoza [48], a bimodal distribution typically emerges from the merging of two unimodal populations, reinforcing the understanding of both micro- or nano-scale fibrils and larger agglomerates within our sample. This issue is a known challenge in nanocellulose production, influenced by aspects like the effectiveness of centrifugation steps [49]. Future endeavors may optimize micro-cellulose properties for hydrogel synthesis by incorporating downstream purification methods, such as extended centrifugation or filtration, to reduce these larger aggregates and achieve a more uniform cellulose dispersion.

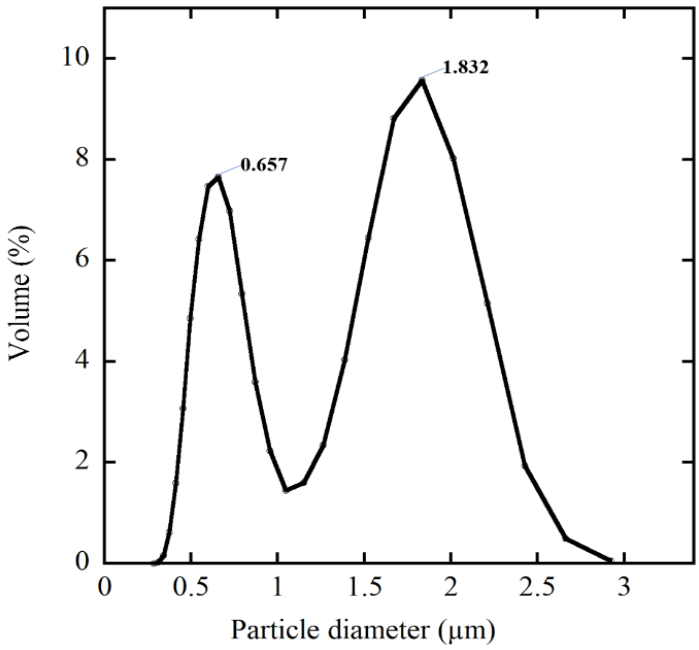

Figure 5 The particle size distribution of the bio-pretreated and purified cellulose.

Hydrogel and characterization

This study synthesized the hydrogel by grafting, which effectively crosslinks cellulose fibers with additional polymeric components using a chemical process known as radical polymerization. This approach functions analogously to constructing a three-dimensional scaffold capable of water absorption. Grafting is particularly effective here because it allows the polyacrylamide chains to grow directly from the cellulose hydroxyl groups, forming strong covalent bonds. This intimate chemical linkage ensures that the cellulose acts as an integral part of the polymer network rather than just a filler, significantly enhancing the water absorption capacity of the resulting hydrogel [50]. Initially, the cellulose was subjected to thermal treatment at 95 °C for 30 min, facilitating its dissolution while eliminating any residual lignin or hemicellulose that could interfere with the polymerization process [51]. After lowering the temperature to 60 °C, APS was introduced as an initiator, catalyzing the polymerization between AAm and MBA, the latter serving as a crosslinking agent [52]. MBA is a pivotal connector, creating linkages that establish the hydrogel intricate network structure, enhancing its water retention capabilities [53]. Following the polymerization reaction, a purification step was performed to remove unreacted monomers and other impurities, yielding 3.14 g of hydrogel from just 1 g of cellulose. Such a considerable conversion demonstrates the power of this method to turn cellulose from agricultural waste into a functional, water-absorbing biomaterial, which is a very valuable material in medicine and agriculture.

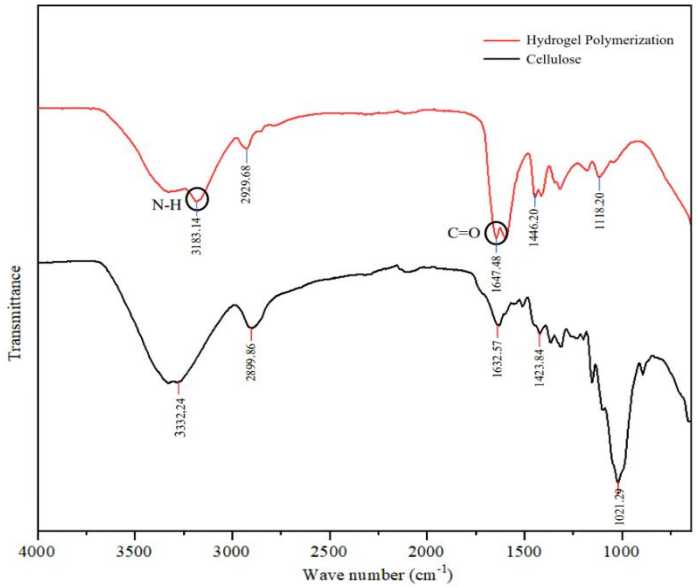

Figure 6 FTIR spectral comparison between cellulose and the resulting cellulose-acrylamide hydrogel composite.

FTIR analysis of the synthesized hydrogels manifests significant alterations in the chemical structure due to the interaction between cellulose and the polyacrylamide matrix. **Figure 6** describes the FTIR spectra exhibiting characteristic absorption bands for cellulose and hydrogel, with peaks around 3,300 cm^{-1} corresponding to the hydroxyl (–OH) groups and those below 2,900 cm^{-1} indicating C–H stretching vibrations. Notably, the spectrum of the hydrogel composite displays a distinct band at 3,183.14 cm^{-1}, attributed to N-H stretching vibrations from the polyacrylamide and an additional peak at 1,647.48 cm^{-1} associated with the C=O functional group of the amide linkages formed during grafting. These peaks signify the successful incorporation of polyacrylamide into the cellulose matrix, indicating that the copolymerization process through grafting and crosslinking has effectively occurred [54,55]. Furthermore, the disappearance of the prominent C–O peak in the cellulose spectrum suggests a transformation of the cellulose structure into a more complex hydrogel framework during the synthesis process [16,56].

The presence of the new functional groups in the FTIR spectrum confirms the successful modification of cellulose to enhance the hydrogel properties, suggesting their potential in various applications. Specifically, the amide group indicates that the resulting hydrogels can offer improved mechanical properties, bioactivity and responsiveness to environmental stimuli [57,58]. These modifications contribute to the hydrogel structural integrity and performance and signify its suitability for drug delivery and tissue engineering [59]. By establishing apparent differences between the spectra of cellulose and the hydrogel composites, FTIR analysis helps validate the effective integration of polyacrylamide in the hydrogels, laying the groundwork for future studies focusing on tailored functionalities for enhanced therapeutic applications.

The swelling behavior of the synthesized hydrogel was thoroughly investigated, highlighting the hydrogel capacity to absorb and retain water effectively, as indicated in **Figure 7**.

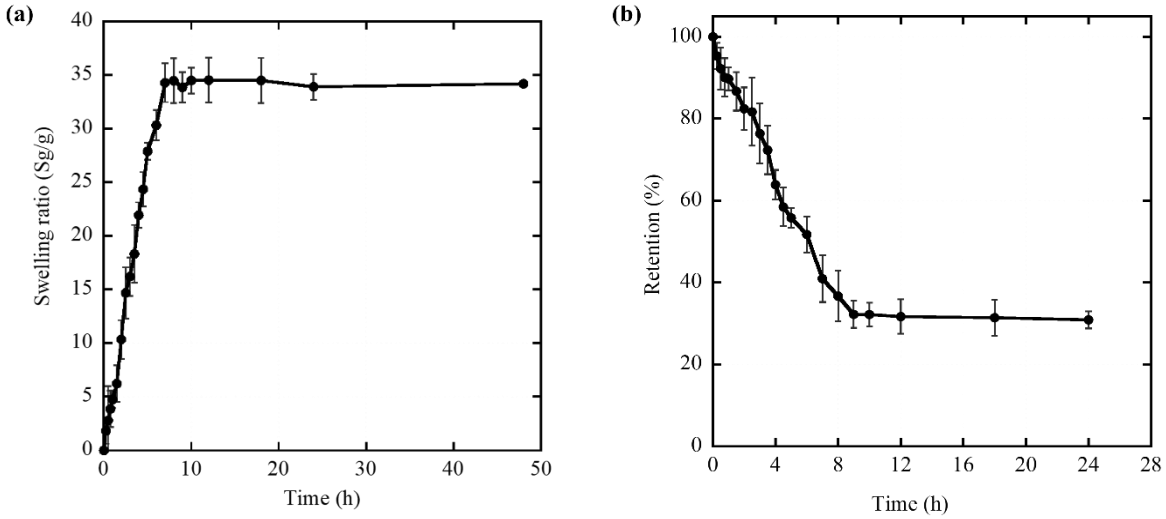

Figure 7 Swelling ratio (a) and (b) and water retention of the hydrogel as a function of immersion times at room temperature.

The evolution of the swelling ratio, as depicted in **Figure 7(a)**, illustrates a significant increase in hydrogel weight upon immersion in distilled water, showing an exponential trend during the initial 6 h. During this phase, the swelling ratio gradually increased, plateauing near a constant Sg/g value of approximately 34, indicating that the hydrogel reached a saturation point. This result suggests the network can effectively accommodate water molecules due to its crosslinked structure. It is crucial for moisture retention applications such as wound dressings or drug delivery systems [60].

Furthermore, the water retention capability of these hydrogels was evaluated, as shown in **Figure 7(b)**, revealing that the material maintained significant water content under similar osmotic pressure conditions even after 10 h. This endurance is essential as it demonstrates the hydrogel ability to preserve hydration and sustain its functional properties over time, which is vital for biological applications [61]. The results indicate that the hydrogel can effectively balance swelling and water retention, showcasing its potential for various biomedical and material applications requiring consistent hydrophilicity and moisture retention [62].

Absorption and release of vitamin C by hydrogel

The results of absorption and release tests are presented in **Figure 8**, showing the trends for 48 h for absorption and 24 h for release experiments. The absorption profile of ascorbic acid (AAc), representing vitamin C in the produced hydrogel, was monitored over 48 h, as shown in **Figure 8(a)**. Characterized by a significant swelling capacity, the hydrogel achieved a maximum swelling ratio (Sg/g) of 34 within the first 8 h. The kinetics of AAc absorption are notably correlated with this swelling behavior. A rapid initial uptake of AAc was observed, with concentrations in the hydrogel increased from approximately 8.32 %w/w at 6 h to about 18.44 %w/w at 12 h. This trend indicates that as the hydrogel expands, it effectively entraps the surrounding AAc solution, facilitating efficient absorption [63]. The optimal absorption timeframe for AAc appears to be between 6 and 24 h, after which the uptake rate significantly diminishes. During examination, the concentration gradually increased to approximately 18.88 %w/w, reaching a plateau of 12 to 48 h. This plateau suggests that the hydrogel has attained its equilibrium state for AAc absorption under the rinsing conditions employed, reached the equilibrium within 18 h and its subsequent sustained up to 24 h, highlighting that extending the rinsing time beyond 24 h yields minimal additional benefits in terms of increasing AAc concentration within the hydrogel.

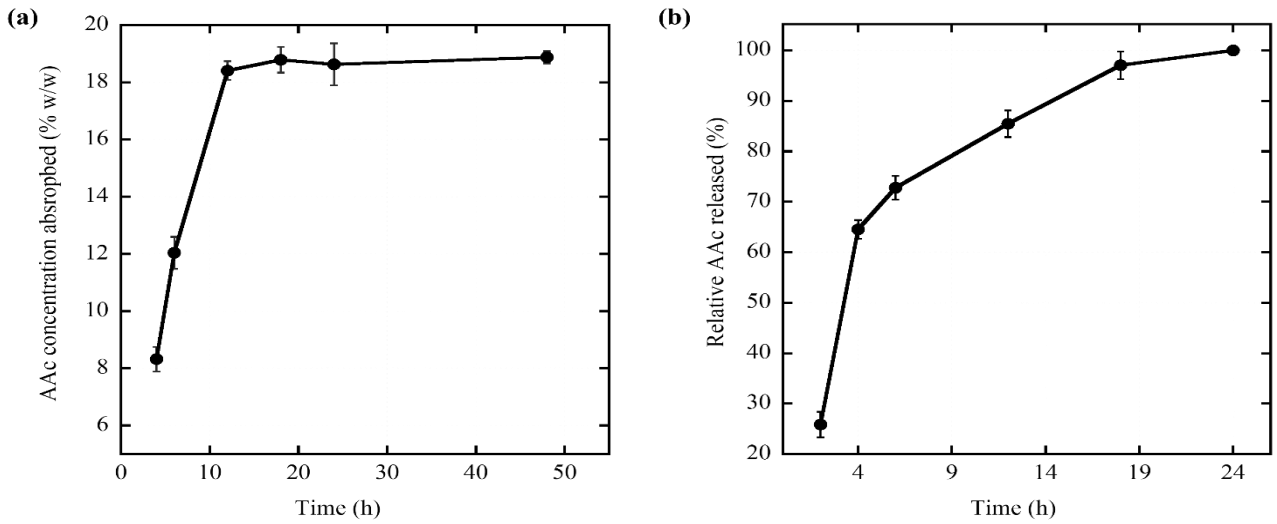

Figure 8 Concentration of AAc absorbed (a) and concentration of AAc released (b), by hydrogel as a function of time.

The efficient loading of AAc during the maximum swelling period is critical, underscoring its potential for applications in vitamin delivery systems. Previous studies indicate that hydrogel loading capacity can significantly influence encapsulated nutrient release dynamics, including ascorbic acid [64]. Hydrogel formulations containing AAc enhance delivery efficacy and improve stability and bioavailability in physiological environments [65]. Given the essential roles of vitamin C in biological processes, including its antioxidant properties and contribution to collagen synthesis, the development of such hydrogels has important implications for nutritional and therapeutic applications [66].

Figure 8(b) represents the data on AAc release from the swelling-hydrogel matrix. The observed release profile of ascorbic acid (AAc) from the hydrogel over 24 h exhibits in two patterns, initially, a rapid burst release occurs within the first 4 h, during which approximately 64% of the loaded AAc is released, a phenomenon indicative of a significant proportion of AAc being situated near the surface of the hydrogel or being weakly bound within the polymer network, thus allowing for quick diffusion into the surrounding medium [67]. Subsequently, from 4 h to 24 h, the release rate slows considerably and by the end of the 24 h, nearly 100% of the initially loaded AAc has been released, suggesting that the AAc trapped deeper within the hydrogel matrix requires a longer time for diffusion, likely due to tortuous pathways within the crosslinked structure. Consequently, this biphasic release pattern confirms the hydrogel potential for applications requiring both an initial rapid delivery of vitamin C and a sustained release over a longer duration, as the initial burst can provide immediate therapeutic effects, while the subsequent gradual release helps maintain the desired concentration over time; such controlled release mechanisms are critical in developing effective drug delivery systems, as they can enhance the bioavailability and stability of hydrophilic drugs, including nutrients like vitamin C [68,69].

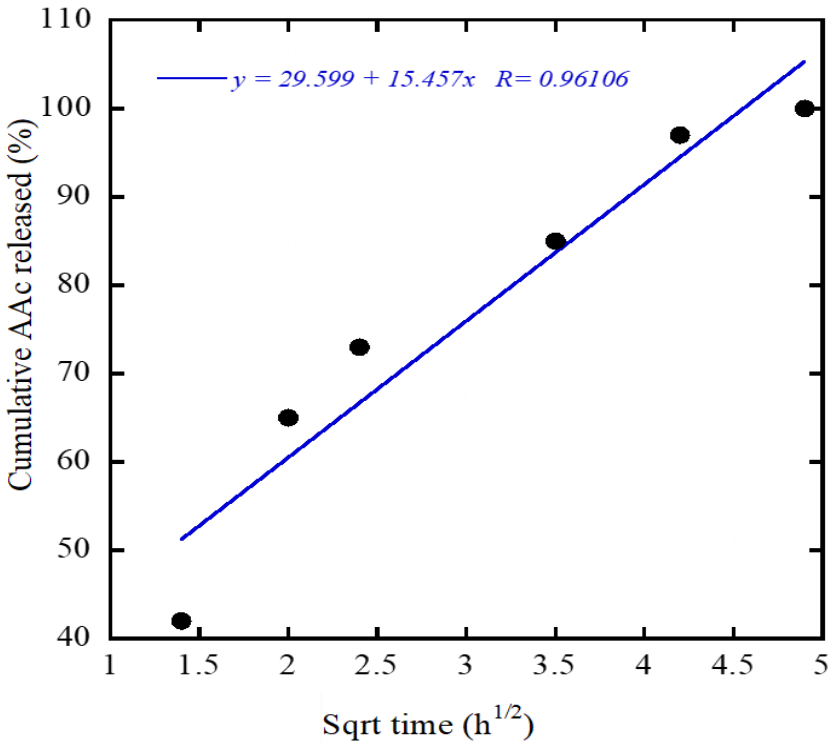

Figure 9 Presents the Higuchi kinetic plot, illustrating the cumulative percentage of AAc released from the hydrogel over time, expressed as a function of the square root of time.

Figure 9 describes the release of AAc from the hydrogel demonstrating strong linearity against the square root of time ($R^2 = 0.961$), indicating its adherence to the Higuchi model, where diffusion is the dominant release mechanism. From the regression equation (y = 29.599 + 15.457x), the Higuchi dissolution constant (k_H) was determined to be 15.457, quantifying the rate of AAc diffusion through the hydrogel matrix. This k_H value is consistent with existing literature, such as Mir *et al*. [70] report of 14.7 for metformin release from cellulose-acrylamide. The observed initial burst release (29.599%) is also typical for hydrogel systems with hydrophilic drugs, as highlighted by Zhang *et al.* [71]. This initial rapid release, followed by diffusion-controlled kinetics, is a common characteristic of hydrogel-based drug delivery systems.

Antibiotic absorption and release assay by hydrogel

In this experiment, a susceptibility test of amoxicillin to *E. coli* and *S. aureus* was applied as a laboratory procedure to determine whether these bacteria are likely to be inhibited or killed by amoxicillin, a commonly used penicillin-type antibiotic. The standard Kirby-Bauer disk diffusion assay was adapted using a weighted piece of antibiotic-impregnated hydrogel instead of the conventional disk. The evaluation of susceptibility refers to the Clinical and Laboratory Standards Institute (CLSI), even though the concentration of the antibiotic solution used to impregnate the hydrogel was made higher than standard (10 µg/mL) to evaluate the release of amoxicillin in the diffusion method.

Figure 10 shows the examination result in a modified Kirby-Bauer disk diffusion assay, showing the formation of clear zones for both bacterial strains tested.

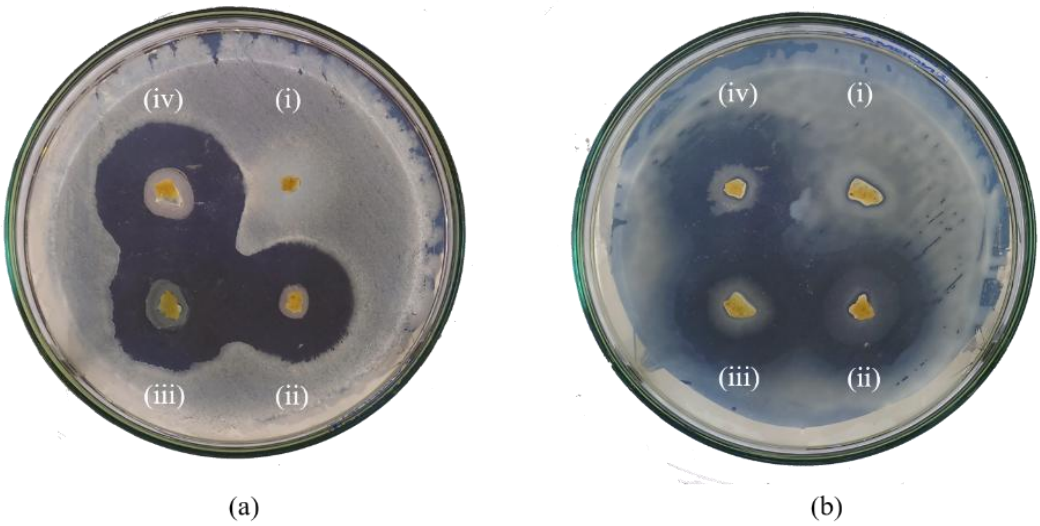

Figure 10 Antimicrobial susceptibility testing against (a) *E. coli* and (b) *S. aureus* using hydrogels containing amoxicillin at concentrations of (i) 0, (ii) 25, (iii) 50 and (iv) 100 µg/mL, respectively.

The formation of clear zones of inhibition around both *E. coli* (a) and *S. aureus* (b) indicated their susceptibility to amoxicillin based on established interpretive criteria for zone diameter (CLSI). The efficacy of amoxicillin against both bacterial strains was evident across the tested concentrations (25, 50 and 100 µg/mL), as demonstrated by the clear zones of inhibition. *E. coli* exhibited clear zones with diameters of 23, 25 and 27 mm, while *S. aureus* displayed zones with diameters of 24, 26 and 30 mm, respectively, showcasing an apparent dose-dependent inhibitory effect. In this assay, *S. aureus* consistently shows a larger inhibition zone at each tested concentration than *E. coli*. These results suggest that, under these testing conditions, *S. aureus* might be more susceptible to amoxicillin than the *E. coli* strain.

The swelling capacity of the hydrogel plays a crucial role in its ability to load and release substances, including antibiotics like amoxicillin. Several studies support this relationship between swelling behavior and drug release mechanisms. For instance, Gao [57] demonstrated that hydrogels with higher swelling ratios could accommodate more drug molecules, resulting in improved delivery efficiency of therapeutic agents such as antibiotics. Similarly, Simancas [72] and Tang [73] highlighted the significant influence of swelling capacity on the diffusion kinetics of drugs within hydrogel matrices, as the swelling facilitates the formation of channels that ease the escape of the loaded substances. Furthermore, researchers [74-76] published that a well-optimized swelling capacity in hydrogels can lead to a controlled and sustained release of antibiotics, thereby enhancing their therapeutic efficacy and reducing the need for frequent dosing. This behavior is particularly advantageous in combating infections, as it allows for prolonged exposure of pathogens to the antimicrobial agents.

Conclusions

The results obtained from this study demonstrate the promising potential of pineapple waste as a source of cellulose, based on its cellulose content, which reaches 38.5%. A mangrove-derived actinomycete isolate, ActM-DMB 7, exhibits preferential xylanolytic activity, which can be utilized for bio-pretreatment to obtain cellulose from pineapple waste. Subsequently, successful hydrogel synthesis was achieved by grafting acrylamide onto the refined cellulose, confirmed by the presence of characteristic N-H (3,183.14 cm^{-1}) and C=O (1,647.48 cm^{-1}) amide bands in FTIR analysis. The resulting hydrogels demonstrated significant swelling capacity, reaching a plateau of around 34 g/g and maintained substantial water retention over 10 h. Furthermore, in the AAc absorption application, the hydrogel has absorption capacity equilibrium within 18 h and its subsequent sustained release of AAc over 24 h. The other application of antibiotic loading, using amoxicillin, demonstrated apparent dose-dependent

antibacterial activity against *E. coli* and *S. aureus*. This research highlights the potential of utilizing pineapple core waste to synthesize functional hydrogels with biomedical applications. It contributes to a circular economy model, promoting sustainability and generating economic value from biomass byproducts.

Acknowledgements

This study was conducted using the Research Innovation Collaboration project funding under contract number 9949/UN26/HK.01.03/2022 for Heri Satria, supported by the Higher Education Technology and Innovation (HETI) Project, University of Lampung, Indonesia. The authors would like to thank PT Bromelain Enzyme for generously supplying the pineapple waste, which was essential for the successful completion of this study.

Declaration of Generative AI in Scientific Writing

The authors declare they have not used Artificial Intelligence (AI) tools in creating this article.

CRediT author statement

Heri Satria: Conceptualization, Methodology, Validation, Formal analysis, Resources, Data curation, Writing- Original draft, Writing- Review and Editing, Visualization, Supervision, Funding acquisition.

Kamisah Delilawati Pandiangan: Conceptualization, Methodology, Validation, Resources, Data curation, Writing- Review and Editing, Supervision.

Hapin Afriyani: Conceptualization, Resources, Data curation.

Diska Indah Alista: Software, Formal analysis, Investigation, Resources, Data curation, Writing- Original draft, Writing- Review and Editing, Project administration.

Arifah Rara Afiria: Software, Formal analysis, Investigation, Resources, Writing- Original draft.

Febiana Nabila: Software, Formal analysis, Investigation, Resources, Writing- Original draft.

References

[1] MS Birajdar, H Joo, WG Koh and H Park. Natural bio-based monomers for biomedical applications: A review. *Biomaterials Research* 2021; **25**, 8.

[2] S Janjić, M Kostić, P Škundrić, B Lazić and J Praskalo. Antibacterial fibers based on cellulose and chitosan. *Contemporary Materials* 2013; **2(3)**, 207-218.

[3] X Fan, Z Xiong, J Li, J Lin and X Li. A biodegradable cellulose fibrous membrane comprising cellulose microfibers and nanofibrils with enhanced interaction through crosslinking structure. *Polymers for Advanced Technologies* 2023; **34(9)**, 3022-3034.

[4] J Zhang, Y Qi, Y Shen and H Li. Research progress on chemical modification and application of cellulose: A review. *Materials Science - Medžiagotyra* 2022; **28(1)**, 60-67.

[5] V Miljković, I Gajić and L Nikolić. Waste materials as a resource for production of CMC superabsorbent hydrogel for sustainable agriculture. *Polymers* 2021; **13(23)**, 4115.

[6] S Punyanunt, P Nanta and R Puttipan. Green-chemical nanofibrillated cellulose from pineapple cores using microfluidization. *Trends in Sciences* 2024; **22(2)**, 9085.

[7] TLR Corrêa, AT Júnior, LD Wolf, MS Buckeridge, LVD Santos and MT Murakami. An actinobacteria lytic polysaccharide monooxygenase acts on both cellulose and xylan to boost biomass saccharification. *Biotechnology for Biofuels* 2019; **12**, 117.

[8] H Satria, Yandri, Nurhasanah, S Yuwono and D Herasari. Extracellular hydrolytic enzyme activities of indigenous actinomycetes on pretreated bagasse using choline acetate ionic liquid. *Biocatalysis and Agricultural Biotechnology* 2020; **24**, 101503.

[9] H Enawgaw, T Tesfaye, KT Yilma and D Limeneh. Synthesis of a cellulose-co-amps hydrogel for personal hygiene applications using cellulose extracted from corncobs. *Gels* 2021; **7(4)**, 236.

[10] MO Haque and MIH Mondal. Synthesis and characterization of cellulose-based eco-friendly

hydrogels. *Rajshahi University Journal of Science and Engineering* 2016; **44**, 45-53.

[11] H Abdelhamid and A Mathew. Cellulose-based nanomaterials advance biomedicine: A review. *International Journal of Molecular Sciences* 2022; **23(10)**, 5405.

[12] Q Guan, H Yang, Z Han, Z Ling, C Yin, K Yang, Y Zhao and S Yu. Sustainable cellulose-nanofiber-based hydrogels. *ACS Nano* 2021; **15**, 7889-7898.

[13] H Jin, M Kettunen, A Laiho, H Pynnonen, J Paltakari, A Marmur, O Ikkala and R Ras. Superhydrophobic and superoleophobic nanocellulose aerogel membranes as bioinspired cargo carriers on water and oil. *Langmuir* 2011; **27(5)**, 1930-1934.

[14] G Priya, B Madhan, U Narendrakumar, RK Suresh and I Manjubala. *In vitro* and *in vivo* evaluation of carboxymethyl cellulose scaffolds for bone tissue engineering applications. *ACS Omega* 2021; **6(2)**, 1246-1253.

[15] H Risite, M Salim, B Oudinot, E Ablouh, H Joyeux, H Sehaqui, J Razafimahatratra, A Qaiss, ME Achaby and Z Kassab. *Artemisia annua* stems a new sustainable source for cellulosic materials: Production and characterization of cellulose microfibers and nanocrystals. *Waste and Biomass Valorization* 2022; **13(4)**, 2411-2423.

[16] K Nakasone and T Kobayashi. Effect of pretreatment of sugarcane bagasse on the cellulose solution and application for the cellulose hydrogel films. *Polymers for Advanced Technologies* 2016; **27(7)**, 973-980.

[17] TK Ghose. International union of pure and applied chemistry applied chemistry division commission on biotechnology measurement of cellulase activities. *Pure and Applied Chemistry* 1987; **59(2)**, 257-268.

[18] MJ Bailey, P Biely and K Poutanen. Interlaboratory testing of methods for assay of xylanase activity. *Journal of Biotechnology* 1992; **23(3)**, 257-270.

[19] GL Miller. Use of dinitrosalicylic acid reagent for determination of reducing sugar. *Analytical Chemistry* 1959; **31(3)**, 426-428.

[20] H Dai and H Huang. Enhanced swelling and responsive properties of pineapple peel carboxymethyl cellulose-g-poly(acrylic acid-co-acrylamide) superabsorbent hydrogel by the introduction of carclazyte. *Journal of Agricultural and Food Chemistry* 2017; **65(3)**, 565-574.

[21] L Abe-Matsumoto, YA de Araújo and MM Leite. Stability of vitamin C in enriched jelly. *Brazilian Journal of Analytical Chemistry* 2020; **7(27)**, 14-19.

[22] Z Marjanović-Balaban, V Antunović and D Jelić. Determination of vitamin C content in dietary supplements. *Quality of Life* 2014; **5(3-4)**, 87-92.

[23] V Friuli, S Pisani, B Conti, G Bruni and L Maggi. Tablet formulations of polymeric electrospun fibers for the controlled release of drugs with pH-dependent solubility. *Polymers* 2022; **14(10)**, 2127.

[24] AVT Figueroa, CJP Martinez, TC Castro, EB Martinez, MAGC Madueno, AMG Alegria, TL Ceniceros and LA Villegas. Composite hydrogel of poly(acrylamide) and starch as potential system for controlled release of amoxicillin and inhibition of bacterial growth. *Journal of Chemistry* 2020; **2020(1)**, 860487.

[25] ALT Benatti and MLTM Polizeli. Lignocellulolytic biocatalysts: The main players involved in multiple biotechnological processes for biomass valorization. *Microorganisms* 2023; **11(1)**, 162.

[26] T Miyamoto, R Takada, Y Tobimatsu, Y Takeda, S Suzuki, M Yamamura, K Osakabe, Y Osakabe, M Sakamoto, and T Uzemawa. OsMYB108 loss-of-function enriches p-coumaroylated and tricin lignin units in rice cell walls. *The Plant Journal* 2019; **98(6)**, 975-987.

[27] JS Poulsen, WV Macêdo, T Bonde and J Nielsen. Energetically exploiting lignocellulose-rich residues in anaerobic digestion technologies: From bioreactors to proteogenomics. *Biotechnology for Biofuels and Bioproducts* 2023; **16**, 183.

[28] E Schmitz, KE Nordberg and P Adlercreutz. Warming weather changes the chemical composition of oat hulls. *Plant Biology* 2020; **22(6)**, 1086-1091.

[29] L Varriale, M Volkmar, J Weiermüller and R Ulber. Effects of pretreatment on the biocatalysis of renewable resources. *Chemie Ingenieur Technik* 2022; **94(11)**, 1818-1826.

[30] L Fitri, Y Yurnita and S Suhartono. Isolation and cellulolytic activity assay of actinobacteria isolated from palm oil wastewater. *Trends in Sciences* 2023; **20(6)**, 6715.

[31] X Cao, F Li, Y Li, S Chen, X Li and Y Lu. Preparation and application of cellulose-based hydrogels derived from bamboo. *ChemRxiv* 2022. https://doi.org/10.26434/chemrxiv-2022-134z8

[32] AS Patri, R Mohan, Y Pu, C Yoo, A Ragauskas, R Kumar, D Kisailus, C Cai and C Wyman. THF co-solvent pretreatment prevents lignin redeposition from interfering with enzymes yielding prolonged cellulase activity. *Biotechnology for Biofuels* 2021; **14**, 63.

[33] J Wang, J Liang, Y Li, L Tian and Y Wei. Characterization of efficient xylanases from industrial-scale pulp and paper wastewater treatment microbiota. *AMB Express* 2021; **11**, 19.

[34] H Andaleeb, N Ullah, S Falke, M Perbandt, H Brognaro and C Betzel. High-resolution crystal structure and biochemical characterization of a GH11 endoxylanase from *Nectria haematococca*. *Scientific Reports* 2020; **10(1**), 15658.

[35] MS Mafa, S Malga, A Bhattacharya, K Rashamuse and BI Pletschke. The effects of alkaline pretreatment on agricultural biomasses (corn cob and sweet sorghum bagasse) and their hydrolysis by a termite-derived enzyme cocktail. *Agronomy* 2020; **10(8)**, 1211.

[36] K Kojima, N Sunagawa, Y Yoshimi, T Tryfona, M Samejima, P Dupree and K Igarashi. Acetylated xylan degradation by glycoside hydrolase family 10 and 11 xylanases from the white-rot fungus: *Phanerochaete chrysosporium*. *Journal of Applied Glycoscience* 2022; **69(2)**, 35-43.

[37] A Procentese, ME Russo, SI Di and A Marzocchella. Kinetic characterization of enzymatic hydrolysis of apple pomace as feedstock for a sugar-based biorefinery. *Energies* 2020; **13(5)**, 1051.

[38] A Xia, C Zhang, T Zhu, K Lin, D Zhang, Y Huang, X Zhu and Q Liao. Nature-inspired bioreactor for enzymatic hydrolysis of non-newtonian biomass slurry: A numerical study. *Industrial & Engineering Chemistry Research* 2025; **64(5)**, 3004-3013.

[39] GHD Tonoli, K Holtman, LE Silva, D Wood, L Torres, T Williams, J Oliveira, A Fonseca, A Klamczynki, G Glenn and W Orts. Changes on structural characteristics of cellulose pulp fiber incubated for different times in anaerobic digestate. *Cerne* 2021; **27**, e-102647.

[40] A Merlini, C Claumann, AW Zibetti, A Coirolo, T Rieg and R Machado. Kinetic study of the thermal decomposition of cellulose nanocrystals with different crystal structures and morphologies. *Industrial & Engineering Chemistry Research* 2020; **59(30)**, 13428-13439.

[41] AL López, AS Hernández, MC Cruz, YG Huante, J Campos, JI Bustos, MR Marsch, RC Cano, CC Benitez and LM Hidalgo. TtCel7A: A native thermophilic bifunctional cellulose/xylanase exoglucanase from the thermophilic biomass-degrading fungus thielavia terrestris co3bag1 and its application in enzymatic hydrolysis of agroindustrial derivatives. *Journal of Fungi* 2023; **9(2)**, 152.

[42] Y Zhou, P Zhan, D Tong, W Zhang, Y Qing, Y Huang, L Zhang and J Chen. Deconstruction of poplar wood using peracetic acid and $FeCl_3$ in hot water. *ChemistrySelect* 2022; **7(3)**, e202104019.

[43] MNL Flores, JJC Rodríguez, BA Tamayo, VJ Hernandez, PJ Chanona, CS Gallegos, HH Hernandez and EL Jarquin. Windmill grass (*Chloris spp*.) as a non-wood source of cellulose for reinforcement of starch films. *Polymer Composites* 2024; **45(18)**, 16898-16915.

[44] Q Wang, S Xiao and SQ Shi. The effect of hemicellulose content on mechanical strength, thermal stability and water resistance of cellulose-rich fiber material from poplar. *BioResources* 2019; **14(3)**, 5288-5300.

[45] D Floudas, L Gentile, E Andersson, SG Kanellopoulos, A Tunlid, P Persson and U Olsson. X-Ray scattering reveals two mechanisms of cellulose microfibril degradation by filamentous fungi. *Applied and Environmental Microbiology* 2022; **88(17)**, e0099522.

[46] M Ioelovich. Specific features of enzymatic hydrolysis of cellulose. *World Journal of*

Advanced Research and Reviews 2024; **22(1)**, 381-392.

[47] Z Yang and Q Chen. Enzymatic preparation and characterization of honey pomelo peel cellulose and its cellulose nanofibers. *Industrial Crops and Products* 2023; **206**, 117655.

[48] MH Ramirez, LM Valdez, GT Van and C Lutz. Continuous flow synthesis of zeolite FAU in an oscillatory baffled reactor. *Journal of Advanced Manufacturing and Processing* 2020; **2(2)**, e10038.

[49] PA Larsson, AV Riazanova, CG Cinar, R Rojas, H Ovrebo, L Wagberg and L Berglund. Towards optimised size distribution in commercial microfibrillated cellulose: A fractionation approach. *Cellulose* 2019; **26(3)**, 1565-1575.

[50] A Suo, J Qian, Y Yao and W Zhang. Synthesis and properties of carboxymethyl cellulose-graft-poly (acrylic acid-co-acrylamide) as a novel cellulose-based superabsorbent. *Journal of Applied Polymer Science* 2007; **103(3)**, 1382-1388.

[51] H Wang, X Wang and D Wu. Recent advances of natural polysaccharide-based double-network hydrogels for tissue repair. *Chemistry-An Asian Journal* 2022; **17(17)**, e202200659.

[52] S Buonvino, M Ciocci, D Seliktar and S Melino. Photo-polymerization damage protection by hydrogen sulfide donors for 3D-cell culture systems optimization. *International Journal of Molecular Sciences* 2021; **22(11)**, 6095.

[53] S You, Z Zha, J Li, W Zhang, Z Bai, Y Hu, X Wang, Y Chen, J Wang and H luo. Improvement of XYL10C_Δ N catalytic performance through loop engineering for lignocellulosic biomass utilization in feed and fuel industries. *Biotechnology for Biofuels* 2021; **14**, 195.

[54] R Banat, M Al-Rawashdeh and M Aljnaid. Thermal properties of olive pomace filled linear low density polyethylene bio-composites. *Journal of Macromolecular Science* 2021; **60(11)**, 957-969.

[55] GON Soares, RRL Machado, MM Diniz and AB Silva. Electrospun progesterone-loaded cellulose acetate nanofibers and their drug sustained-release profiles. *Polymer Engineering and Science* 2020; **60(12)**, 3231-3243.

[56] X Liu, J Shen, Y Wang, M Li and S Fu. Photoinduced metal-free atom transfer radical polymerization for the modification of cellulose with poly(n-isopropylacrylamide) to create thermo-responsive injectable hydrogels. *International Journal of Molecular Sciences* 2024; **25(5)**, 2867.

[57] Z Gao, Z Yu, C Huang, L Duan and G Gao. Carboxymethyl cellulose reinforced poly(vinyl alcohol) with trimethylol melamine as a chemical crosslinker. *Journal of Applied Polymer Science* 2017; **134(11)**, 44590.

[58] E Pinho and G Soares. Cotton-hydrogel composite for improved wound healing: Synthesize optimization and physicochemical characterization-part 1. *Polymers for Advanced Technologies* 2018; **29(12)**, 3114-3124.

[59] T Yang, X Li, N Xu, Y Guo, G Liu and J Zhao. Preparation of cellulose nanocrystals from commercial dissolving pulp using an engineered cellulase system. *Bioresources and Bioprocessing* 2023; **10**, 42.

[60] C Zhang, Y Qi and Z Zhang. Swelling behavior of polystyrene microsphere enhanced PEG-based hydrogels in seawater and evolution mechanism of their three-dimensional network microstructure. *Materials* 2022; **15(14)**, 4959.

[61] N Sarvesh, K Afeeza, V Suresh and E Dilipan. Development of the antioxidant property of seagrass extract-based hydrogel for dental application. *Cureus* 2024; **16(2)**, e54544.

[62] S Park, Y Son, J Park, S Lee, N Kim, S Jang, T Kang, J Song and G Khang. Polydeoxynucleotide-loaded visible light photo-crosslinked gelatin methacrylate hydrogel: Approach to accelerating cartilage regeneration. *Gels* 2025; **11(1)**, 42.

[63] ES Santana, LB Leal, LA Silva, ICF Barbosa, CML Melo, DKDN Santos and JRC Vieira. Association of *Rhizophora mangle* and ascorbic acid in hydrogels: Evaluation of cytotoxic and immunomodulatory effects. *Brazilian Journal of Pharmaceutical Sciences* 2023; **59(2)**, e20179.

[64] ME Trejo-Caballero, L Díaz-Patiño, M González-Reynac, G Molina, J Lopez-Miranda, R Esparza, B Espana-Sanchez, N Arjona and M Estevez. Biopolymeric hydrogel electrolytes obtained by using natural polysaccharide–poly(itaconic acid-

co-2-hydroxyethyl methacrylate) in deep eutectic solvents for rechargeable Zn–air batteries. *Green Chemistry* 2023; **25(17)**, 6784-6796.

[65] PM Rastegar, I Tahir, B Garcia-Bailo, K Lo, K Jarvi and AE Sohemy. Ascorbic acid is associated with favourable hormonal profiles among infertile males. *Frontiers in Reproductive Health* 2023; **5**, 1143579.

[66] AC Carr and S Rowe. Factors affecting vitamin C status and prevalence of deficiency: A global health perspective. *Nutrients* 2020; **12(7)**, 1963.

[67] M Klučáková. Agarose hydrogels enriched by humic acids as the complexation agent. *Polymers* 2020; **12(3)**, 687.

[68] M Bańkosz. Physicochemical characterization and kinetics study of polymer carriers with vitamin C for controlled release applications. *Materials* 2024; **17(22)**, 5502.

[69] NC Silva, CJT Silva, MP Gonçalves and F Borsagli. Carboxymethyl-cellulose-based hydrogels incorporated with cellulose nanocrystals loaded with vitamin D for controlled drug delivery. *Processes* 2024; **12(7)**, 1437.

[70] A Mir, WJ Fletcher, DK Taylor, J Alam and U Riaz. Sustained release studies of metformin hydrochloride drug using conducting polymer/gelatin-based composite hydrogels. *ACS Omega* 2024; **9**, 18766-18776.

[71] S Zhang, G Ge, Y Qin, W Li, J Dong, J Mei, R Ma, X Zhang, C Zhu, W Zhang and D Gang. Recent advances in responsive hydrogels for diabetic wound healing. *Materials Today Bio* 2023; **18**, 100508.

[72] HR Simancas, CA Fernández, BJ Aparicio, K Slowing, JR Rubio, CE Lopez and SA Torres. Controlled release of highly hydrophilic drugs from novel poly(magnesium acrylate) matrix tablets. *Pharmaceutics* 2020; **12(2)**, 174.

[73] Z Tang, Y Yang, Y Pan, M Yu, X Lin and A Mondal. Biocompatible, injectable and self-healing poly(n-vinylpyrrolidone)/carboxymethyl cellulose hydrogel for drug release. *ACS Omega* 2024; **9(5)**, 5854-5861.

[74] NR Karakuş, S Türk, EG Guney, M Syzdykbayev, N Appazov and M Ozacar. Investigation of tannic acid crosslinked PVA/PEI-based hydrogels as potential wound dressings with self-healing and high antibacterial properties. *Gels* 2024; **10(11)**, 682.

[75] MUA Khan, I Iqbal, MNM Ansari, S Razak, M Raza, A Sajjad, F Jabeen, M Mohamad and N Jusoh. Development of antibacterial, degradable and pH-responsive chitosan/guar gum/polyvinyl alcohol blended hydrogels for wound dressing. *Molecules* 2021; **26(19)**, 5937.

[76] Medha and S Sethi. Chitosan based hybrid superabsorbent for controlled drug delivery application. *Biotechnology Progress* 2024; **40(2)**, e3418.